Contrib Mineral Petrol (1982) 80:140–146

Contributions to Mineralogy and Petrology

Geothermometry and Geobarometry of Plagioclase-Hornblende Bearing Assemblages

L.P. Plyusnina
Institute of Experimental Mineralogy, USSR Acad. Sci., 142432 Chernogolovka, Moscow District, USSR

Abstract. The reaction $Hb + Zo(Ep) + H_2O + CO_2 \rightleftharpoons Pl + Chl + Cc + Q$ was studied under hydrothermal conditions at $P_{total} = 2$, 4, 6 and 8 kb at $X_{CO_2} = 0.1$. The continious transition from tremolite (actinolite) to Al-rich hornblende was fixed along the equilibrium curve of the reaction, providing a complete solid solution in the calcic amphibole series. A dependence of Al content in Ca-amphiboles and coexisting plagioclases on *PT*-conditions of their crystallization, determined for a wide range of temperature (450–650° C) and pressure (2–8 kb), has been used for construction of the experimental geothermobarometer. This may be employed to deduce temperature and pressure conditions of metamorphism of the albite-epidote-amphibolite and the amphibolite facies metabasites, including zoisite (or epidote)-bearing assemblages. An application of the Hb – Pl geothermobarometer is illustrated on the Patom Highland amphibolites and also on the well-known mafic schists of Vermont.

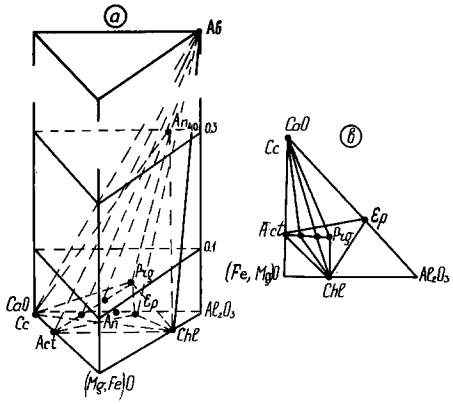

Fig. 1 a, b. $Na_2O - CaO - (Mg, Fe)O - Al_2O_3$-diagram (**a**) and projection of the mineral phases on the $CaO - Al_2O_3 - (Mg, Fe)O$ face of the tetrahedron (**b**), showing the considered mineral assemblage of the amphibolite facies metabasites

Introduction

It is known that amphiboles are a good indicator of temperature and pressure over wide ranges of metamorphic conditions. In due time, Perchuk (1970) had suggested to use the examined dependence of Ca:Na ratio of coexisting amphiboles and plagioclase on T as geothermometer. Besides, there are evidences about increasing Al content of Ca-amphiboles with increasing grade of metamorphism (Leake 1962; Kostyuk 1970; Hietanen 1974; Graham 1974). None the less, Raase (1974) had supposed that "the rather complex dependence of the Al content upon temperature, pressure and chemical environments makes it difficult to use it as an indicator of metamorphism". In this connection, the significance of the experimental study of the variation in the Al content of Ca-amphiboles in dependence on pressure and temperature becomes apparent.

In most world-wide occurrences of mafic greenschist the assemblage of $Ca - Am + Chl + Ep + Ab + Q \pm$ carbonate $\pm$ mica[1] is common and persists from greenschist to amphibolite facies with a considerable change in phase compositions (Shido 1958; Wenk, Keller 1969; Cooper 1972; Laird 1980). With increasing grade Chl and Ep decrease in modal abundance, whilst Am increases, concomitantly Prg and Tsch substitution in these grows. The anorthite content of Pl increases, at first with jump from Ab to Ol (peristerite gap) and then continiously to andesine (Liou et al. 1974). Following Laird (1980), the generalized continious reaction which describes the metamorphism of common mafic schist in the transitional zone is: $X_1Am_1 + Y_1Chl_1 + Ep + Z_1Ab + Q \rightleftharpoons X_2Am_2 + Y_2Chl_2 + Z_2Ol + H_2O$ ($X_2 > X_1$, $Y_2 < Y_1$ and $Z_2 > Z_1$), where the Prg and Tsch substitutions are greater in Am_2 than Am_1.

For graphical representation of this assemblage, including also Cc, the triangular prism with the base $CaO - Al_2O_3$- MgO and Na/Ca + Mg + Al ratio along height was choosen (Fig. 1a). It is seen, that Ca – Ams in result of the lower Na content are located near the prism base. If FeO is absent as a component, the further projection on to the prism base allows to derive the following monovariant reaction: $Hb + Zo + CO_2 \rightleftharpoons Pl + Chl + Cc + Q$ (1) at X_{CO_2} const. As to Hb compositions containing more Al than 1,75 per formula unit, the reaction (1) is transformed to $Hb + H_2O + CO_2 \rightleftharpoons Zo + Pl + Chl + Cc + Q$ (Fig. 1b). Therefore, experimental treatment of this reaction in the simplified system may be very helpful to define the quantitative dependence of Al content in Am and Pl on PT-conditions.

1 Abbreviations used in this paper: Am = amphibole, Hb = hornblende, Act = actinolite, Tr = tremolite, Prg = pargasite, Tsch = tschermakite, Zo-zoisite, Ep = epidote, Pl = plagioclase, Ab = albite, An = anorthite, Ol = oligoclase, Cc = calcite, Chl = chlorite, Q = quartz

0010-7999/82/0080/0140/$1.40

Experimental Procedure

All runs were accomplished in hydrothermal pressure vessels. The accuracy of the temperature measurements using a chromelalumel thermocouple was to $\pm 5°$, the pressures were measured on Bordon gauge and maintained to within ± 50–100 bar. The H_2O-CO_2 fluid composition is fixed within a sealed Pt capsule by a mixture of decomposing oxalic acid and liquid H_2O, which were taken in required weight proportions. Besides, in a few runs X_{CO_2} was controlled by measuring the weight loss of the capsule upon puncturing and then by measuring the weight loss of the capsule upon drying at 110° C. The starting charges contained a mixture of natural Fe-poor Zo, Ab, Chl, Cc and Q (Table 1). Because of the chemical complexity of natural Am, the Tr_{100}-Prg_{100} and Tr_{100}-$Tsch_{60}$ series of solid solutions were synthesized from oxide mixes for a week at 820–840° C and P_{fl} from 5 to 7 kb by using gaseous pressure vessels. The phase compositions of the run products were identified by X-ray diffraction analyses and by optical methods too. Samples, containing more than 97% of modal Am, were used only. To control the chemical composition of synthetic Ca–Am electron microprobe analysis was applied (Table 2).

The experimental study of the reaction (1) was performed using the above listed monovariant assemblage, whilst a dependence of Ca–Am and Pl compositions on PT-parameters above the reaction boundary was treated with the resulting divariant assemblage Am+Pl+Zo+Cc+Q.

The reaction direction in runs was detected by comparing the X-ray peak heights for product and reactant phases. It must be mentioned, that the use of a mix of reactants and products overcame nucleation difficulties and made it possible to approach the equilibrium curve from both sides.

For the determination of the equilibrium Al content of the amphibole present in reaction (1), several starting mixtures were prepared each containing a synthetic amphibole of different composition. Major element concentrations of amphiboles used are listed in Table 2. If the Al content of the starting amphibole was higher than that of the equilibrium amphibole, the coupled reaction of decomposition of starting Hb: $Hb_1+Cc+Q+H_2O \rightleftharpoons Hb_2+Zo+Pl+CO_2$ (2) (so-called reaction of "drifted equilibrium") occurs along with reaction (1). That is why, an additional set of runs using a "double capsule" method was applied too: an unwelded, but clenched inner Pt capsule (d=3 mm) was charged by the aluminous Hb, whereas the low-temperature assemblage: Chl+Ab+Cc+Q was introduced into an external sealed Pt capsule (d=5 mm). At the low-temperature side of the reaction (1) Hb in the inner capsule breaks down to the Chl+Pl+Cc+Q assemblage, and it is not formed in the external capsule. Under the *PT*-conditions, corresponding to the Hb stability field, a production of Hb and disappearance of Chl in the external ampule were observed by both optical and X-ray methods. At the same time the Hb composition within the inner capsule schifts as a result of the reaction (2), where the Hb_1 is more Al-rich than Hb_2. An approach of residual Am compositions in both capsules provides us an additional criterion of an attainment of equilibrium (Table 3).

Residual Am and Pl were analyzed with a "Camebax" electron microprobe. Standards for studied phases were natural homogeneous Hb, Zo and Ab.

Table 1. Chemical compositions of minerals, used as starting material

Oxides	Albite	Zoisite	Epidote	Mg chlorite	Mg–Fe chlorite
SiO_2	68.85	39.39	38.34	32.12	29.32
TiO_2	–	0.09	0.65	0.19	1.21
Al_2O_3	18.25	32.05	20.95	19.53	17.15
Fe_2O_3	0.05	1.80	13.18	–	6.27
FeO	–	0.21	0.53	0.86	14.15
MnO	–	0.02	0.18	0.12	0.30
MgO	0.27	0.30	0.47	31.73	20.69
CaO	0.95	23.57	20.43	0.55	1.46
K_2O	0.34	0.02	0.18	–	0.65
Na_2O	11.10	0.07	0.35	–	0.17
H_2O^+		1.96	2.84	14.33	
H_2O^-	0.21		1.37		9.27
Total	100.02	99.48	99.60	100.43	100.26

Table 2. Chemical compositions of synthetic amphiboles, used as starting material

Index	Content of oxides in weight per cent				
	SiO_2	Al_2O_3	MgO	CaO	Na_2O
A_1	56.37	0.89	23.45	15.05	–
A_2	56.14	3.00	24.90	13.97	1.6
A_3	56.50	5.00	24.07	13.00	–
A_4	53.50	10.00	22.20	13.00	–
A_5	52.80	12.20	20.20	13.00	–
A_6	52.20	9.50	22.50	12.90	1.9
A_7	44.00	16.50	20.30	12.40	3.3

Table 3. Al-content in amphiboles in runs with the monovariant assemblage

No. run	*P* (kb)	*T* (°C)	Duration (days)	Index of starting Am	Al-content in newly-formed amphiboles		
					Al_2O_3 (%)	Al^{1Y}	Al^{Y1}
672	2	440	14	A_1	3.2	0.25	0.25
672a	2	440	14	A_5	4.4	0.54	0.19
666	2	450	20	A_1	4.4	0.28	0.40
756	2	450	28	A_1	4.1	0.37	0.26
752	2	450	10	A_7	9.7	0.95	0.63
676	4	490	22	A_1	5.5	0.54	0.44
676a	4	490	22	A_7	6.5	0.8	0.2
628	4	500	11	A_7	6.7	0.98	0.13
631	4	500	16	A_2	5.5	0.39	0.32
672b	4	500	22	A_5	6.3	0.59	0.41
697	4	500	11	A_2	5.8	0.7	0.15
697a	4	500	11	A_6	8.5	1.06	0.21
654	4	510	12	A_1	7.8	0.7	0.54
654a	4	510	12	A_3	8.5	0.78	0.56
677	4	520	22	A_1	4.9	0.45	0.3
677a	4	520	22	A_6	8.2	0.71	0.5
678	6	530	10	A_1	8.6	0.9	0.44
678a	6	530	10	A_7	13.6	1.48	0.7
722	6	530	20	A_4	11.5	1.1	0.73
749	8	580	12	A_4	13.0	1.18	0.92
750	8	590	12	A_4	13.6	1.18	1.01
764	8	580	20	A_2	12.0	0.94	1.00

The operating conditions were 15 kv accelerating potential, 0,03 microampere sample current, 20 s count time for Na and 10 s as to Ca, Mg, Al, Si and Fe. The electron beam was focused to about 2 μm in diameter. Typically, from 5 to 10 grains for each phase were analyzed. Correction of raw data for drift, background, fluorescence and atomic number effects were done at the same time by the computer program of Bence and Albee. The maximum errors in the analyses was for Na_2O ($\pm 10\%$) in results of evaporation of sodium, for CaO it is within $\pm 5\%$, the other oxides are considered to be $\pm 3\%$ of the amount present. The Am analyses have been recalculated on the basis of 23 oxygen atoms.

Experimental Results

The equilibrium curve of the reaction (1) imitating the boundary between greenschist and albite-epidote-amphibolite facies was delineated on the $P-T$ diagram at $X_{CO_2}=0.1$ (Fig. 2). An intricate character of Am production reaction must be noted. In run products starting Am grains are preserved usually side by side with newly-formed Am: Tr have not been enriched in Al even in long duration runs. Thus, the starting, intermediate and equilibrium compositions may be present in the run products. One set of kinetic experiments of 7, 10, 14 and 20 days duration shows that with increasing run duration the residual equilibrium crystals gradually grow at the expense of the starting and intermediate composition grains. A similar type of reactions including phases of varying composition was described earlier by Fonarev and Korolkov (1980). The Am compositions, being further away from a given initial composition, are considered to have approached the equilibrium more closely. As is seen from Fig. 3, Tables 3 and 4, the equilibrium Am compositions have been received not in the least all runs. Representation of the experimental results over a wide range of temperatures for each isobare (2, 4 and 6 kb) in the plot of Al content in Ams versus T allows to determine the equilibrium Am compositions for the P, T of interest (Fig. 3).

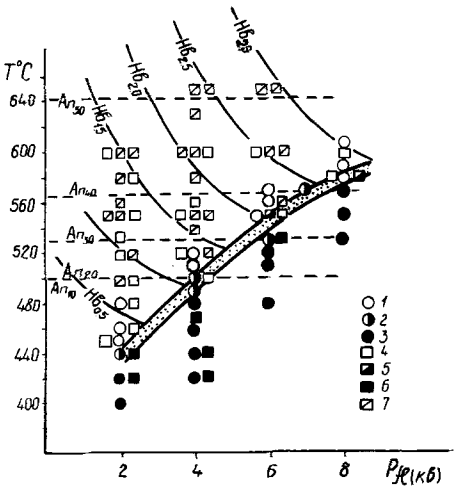

Fig. 2. $P-T$ diagram for the monovariant reaction: $Hb+Zo+CO_2+H_2O=PL+Chl+Cc+Q$ in the iron-free system. Runs with the monovariant assemblage in the $CaO-MgO-Al_2O_3-SiO_2$ system are shown by *circles 1*: Hb grows; *2*: equilibrium; *3*: Chl + Cc + Q grow. *Quadrangles* – runs in the system including also Na_2O: *4*: Hb grows; *5*: equilibrium; *6* the Pl + Chl + Cc + Q stability field; *7* runs with the divariant assemblage Hb + Pl + Zo + Cc + Q

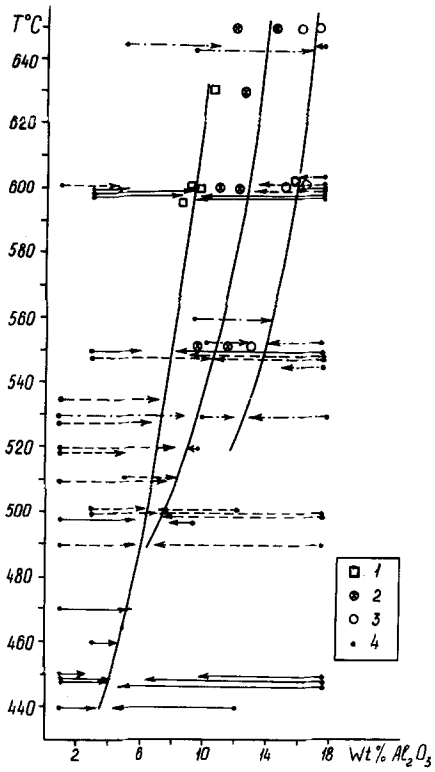

Fig. 3. Plot of Al total versus temperature for Am encountered in this study at $P_{fl}=2$, 4 and 6 kb. A shift of Al content in Am at $P_{fl}=2$ kb is shown by *solid lines*, at 4 kb – by *dashed lines* and at 6 kb – by *dot-dashed lines*. *1–3* – Am, synthesized from the gel mixture: *1*: at 2 kb; *2*: at 4 kb; *3*: at 6 kb; *4*: Al contents in starting Am

The equilibrium compositions at 2, 4 and 6 kb have been used for calculating the dependence of Al content on T by the least-squares method for each isobare:

$$y=-0.00017\,T^2+0.223\,T-61.118 \quad (2\text{ kb}),$$
$$y=-0.00022\,T^2+0.312\,T-91.83 \quad (4\text{ kb}),$$
$$y=-0.00077\,T^2+0.964\,T-283.97 \quad (6\text{ kb}).$$

These equations may be used for extrapolation of experimental data to lower T, that is especially needed for $P>4$ kb.

The experimental results of this paper are referred to the Fe-free system, however, it would be desirable to evaluate the effect of the Fe presence on the recorded phase relations. That is why, Fe-bearing Ams were synthesized from gel mixtures having composition close to tholeiites: the mix N 1 – SiO_2-52.5, Al_2O_3-16.4, FeO-10.3, CaO-9.2, Na_2O-3.8 weight per cent and mix N 2 – SiO_2-48.0, Al_2O_3-12.0, FeO-19.4, MgO-7.1, CaO-11.0, Na_2O-2.0%. Mg–Ams were used as seeds, f_{O_2} was controlled by the Ni–NiO, Mt–Wt and Cu–Cu_2O buffer at $X_{CO_2}=0.1$. The run products were analysed by both X-ray and routine EPMA methods. Results of some runs are represented in the Table 5, where total Fe was calculated as FeO, oxidation ratio was not determined, and Fe:Mg ratio is 100 FeO/(MgO+

Table 4. Am and Pl compositions in runs with the divariant assemblage

No. run	P(kb)	T(°C)	Duration (days)	Index of starting Am	Al content in newly-formed Am			Mole % An in Pl
					Al_2O_3(%)	Al^{IV}	Al^{VI}	
690	2	460	21	A_2	4.8	0.6	0.9	
688	2	470	21	A_2	6.5	0.39	0.62	
738	2	500	20	A_1	5.8	0.57	0.38	10
717	2	500	12	A_7	10.8	0.87	0.85	22
557	2	520	16	A_5	8.5	0.80	0.56	
714	2	550	26	A_7	6.3	0.62	0.36	
725	2	550	14	A_7	8.3	0.87	0.26	
742	2	600	20	A_2	9.5	0.94	0.57	43
759	2	600	20	A_7	9.6	1.14	0.23	43
626	4	500	28	A_7	7.8	0.80	0.40	9
641	4	520	18	A_2	8.2	0.92	0.45	
656a	4	530	12	A_2	6.5	0.80	0.20	
629	4	550	12	A_7	10.6	1.34	0.28	34
673	4	550	22	A_6	10.0	1.02	0.56	38
637	4	550	16	A_2	9.6	1.30	0.52	39
638	4	600	16	A_1	6.4	0.67	0.34	45
698	4	600	11	A_7	13.8	1.17	0.89	46
716	6	550	14	A_4	12.1	1.50	0.80	36
719	6	550	22	A_7	12.6	1.35	0.63	
723	6	560	14	A_6	14.0	1.48	0.77	
720	6	600	14	A_7	15.0	1.60	0.78	
700	6	650	12	A_6	16.8	1.68	1.03	
701	6	650	12	A_3	11.0	0.70	1.64	53

Table 5. Compositions of Am and Pl, synthesized from gel mixture

T(°C)	P(kb)	Buffer	No of starting mixture	Mole % An in Pl	Al content in Am			Fe/Fe+Mg, mole %
					Al_2O_3 (%)	Al^{IV}	Al^{VI}	
600	2	Ni-NiO	1	45	10.1	1.23	0.6	15.0
600	2	Ni-NiO	2	45	9.3	1.21	0.49	73.7
650	2	Ni-NiO	1	45	9.6	1.18	0.59	47.0
550	4	Ni-NiO	2	39	7.1–9.8	0.74	0.93	70.2
600	4	Ni-NiO	1	44	15.1	1.27	1.31	53.6
600	4	Ni-NiO	2	44	10.6–12.4	1.32	0.86	53.0–62.6
600	4	Ni-NiO	2	41	10.8	0.97	0.89	45.0–70.1
630	4	Ni-NiO	1	41	12.3	0.88	1.34	40.0–46.7
650	4	Ni-NiO	1	48	14.7	1.07	1.46	42.7–46.0
600	5	Ni-NiO	1	45	14.6	1.64	0.97	40.5
550	6	Ni-NiO	1	35	12.6	1.10	1.06	46.2
600	6	Ni-NiO	1	39	12.8–16.7	1.37–1.79	1.07–1.22	56.0–64.4
650	6	Ni-NiO	2	46	14.7	1.44	1.09	49.0–55.0
550	4	Cu-Cu_2O	1	36	11.8	0.91	0.9	34.0
550	4	Wt-Mt	1	35	9.2	0.85	0.71	45.8
600	4	Wt-Mt	1	41	14.31	1.50	0.98	51.7

$FeO)_{total}$. The run products, synthesized from gel, also consist of Hb, Pl, Ep, Cc and Q. It must be mentioned that a chemical inhomogeneity of the Fe-bearing Am exists, especially in Mg:Fe ratio, which is easily revealed by EPMA analyses. The compositional variations between differently orientated Am sections and possible reason of those were discussed in the literature before (Grapes 1977). The synthesized Am compositions were plotted also in the diagram of Fig. 3, showing a good consistency with the reported results of experiments, employing the starting monovariant assemblage. It confirms the reliability of these experimental results obtained independently.

In addition, parallel sets of runs with the same Fe-bearing mineral assemblages have been accomplished too. The starting compositions of the natural Chl and Ep are listed in Table 1. The experimental procedure was the same, f_{O_2} was defined by the Ni−NiO buffer. The bulk composition of the starting mixture was constant SiO_2-50.3, Al_2O_3-16.65, MgO-5.9, FeO-9.0, CaO-17.7 and Na_2O-2.5 wt.%. At $T \geqq 530°$ C, most run products show total disappearance of Chl, followed by an intense growth of Hb. Reversibility of the examined reaction has been demonstrated conclusively, for example, at $P=4$ kb, Chl was readily decomposed at $T>490°$ C, while at $T<490°$ C, visible decrease of Am is observed. The equilibrium curve of the reaction (1) in the Fe-bearing system of the reported composition is lo-

Table 6. Chemical compositions of Hb in runs with the divariant assemblage (Fe-bearing system)

PT-conditions	4 kb, 580°		2 kb, 560°		4 kb, 550°		6 kb, 550°	
	1	2	1	2	1	2	1	2
SiO_2	49.0	47.2	50.5	54.3	50.5	51.2	50.8	48.4
Al_2O_3	12.4	12.8	8.4	7.3	10.0	6.3	10.9	11.3
FeO	9.0–17.1	18.9	18.6	4.75	12.4	10.7	16.1	14.9
MgO	8.6–14.8	8.8	10.0	19.5	15.0	18.2	7.4	12.6
CaO	12.0	12.0	11.4	11.8	9.8	9.7	11.3	10.2
Na_2O	0.6	0.6	0.3	1.1	1.6	1.6	1.7	1.9
Total	97.8–99.7	100.3	97.2	98.65	99.3	98.7	98.2	99.3
Si	6.77–6.85	6.89	7.37	7.50	7.1	7.28	7.1	6.9
Al^{IV}	1.23–1.15	1.11	0.63	0.5	0.9	0.72	0.9	1.1
Al^{VI}	0.67–0.78	1.05	0.82	0.68	0.76	0.44	1.0	0.85
Fe^{2+}	1.42–2.3	2.26	2.02	0.55	1.46	1.27	1.91	1.72
Mg	3.25–2.14	1.88	2.17	4.01	3.15	3.86	1.57	2.68
Ca	1.79–1.81	1.75	1.85	1.51	1.5	1.5	1.73	1.56
Na	0.26	0.27	0.08	0.29	0.45	0.45	0.47	0.61

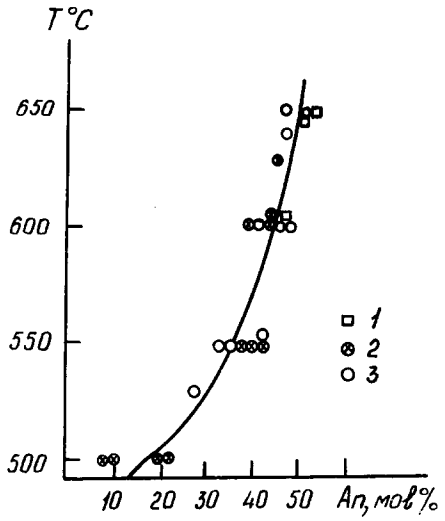

Fig. 4. Plot of An content in Pl (mol %) as a function of temperature at $P_{fl}=2$ kb (*1*), 4 kb (*2*) and 6 kb (*3*)

cated about only 10–15° lower T in comparison with the equilibrium curve depicted in Fig. 2.

As shown in Table 6, the Am equilibrium compositions for the Fe-bearing system have Al contents similar to those from run products in the Mg system and with Am synthesized from gel under the same PT-conditions. It concerns to the Pl compositions also and let us consider that it is succeeded to identify the equilibrium compositions of both Am and Pl. A dependence of the Pl composition on $P-T$ conditions of its formation is illustrated in Fig. 4. The An content is shown to increase with temperature independently of the pressure change. Thus, the plagioclase An content provides a very sensitive indication of temperature for the reported mineral assemblage.

Conclusions

As is seen from Fig. 2, the continious transition from Tr to Al-rich Hb is examined along the equilibrium curve of the reaction (1). It is very important, that continuous increase in P and T have been accompanied by the gradual change of Am composition, providing a complete solid solution in the Ca–Am series. An existence of a miscibility gap in the Act–Hb solid solution is discussed during, at least, the last thirty years. Based on observation of an abrupt transition from Act to Hb in some metamorphic terrains, Shido and Miyashiro (1959), Klein (1969), Cooper (1972) and others had suggested the presence of a miscibility gap between Tr–Act and Hb. On the contrary, Compton (1958), Leake (1962), Grapes (1975) and Graham (1978), considering the inconsistency of a compositional gap between coexisting Act–Hb pairs, had supposed that those do not represent equilibrium pairs, and that a compositional readjustment of the Am to the changing metamorphic conditions was not attained due to a sluggish rate of Am-generating reactions. If this is so, the varied compositional gap ranges within the Ca–Am series are caused by a variation of PT-gradients during either prograde or regrade metamorphism.

The represented experimental results combined with new data of Best (1978) about a continuous transition within Tr–Prg and Tr-edenite solid solution series, an existence of gradual and distinct compositional changes between Act and Hb, the compositional variability in the Ca–Am within the same metamorphic terrain rocks rouse doubt on the reality of the miscibility gap. From this it must follow that presence of coexisting Ca–Am in some metamorphic rocks is being a display of multistage metamorphism, and the compositional gap between associated Act and Hb is larger, the larger a jump of T and P has to occur between various metamorphic stages. So, Hidaka meta-gabbro-amphibolite rocks may be mentioned as an excellent example of occurence of several metamorphic episodes. Grapes (1975) had described there four main stages of progressive metamorphism, characterised by the corresponding changes of the Ca–Am compositions.

Then, the experimentally confirmed significant variation of Al_2O_3 content in Ca–Am with P and T and the change of the Ca/Ca+Na ratio values of Pl in dependence on T may be used as geothermobarometer. The equilibrium compositions of both Ca–Am and Pl for concrete PT-parame-

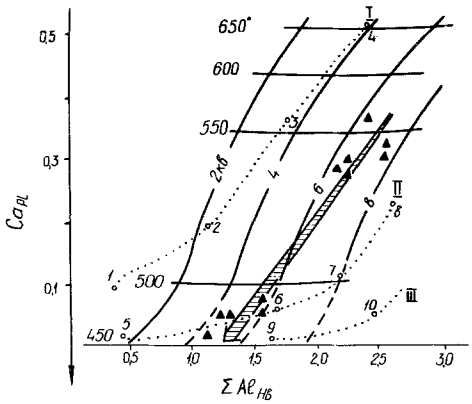

Fig. 5. Experimental Pl–Hb geothermobarometer. Circles and dotted lines represent the zoning of the mafic schists of Vermont after Laird (1980): for figures see text. Assemblages of the Patom Highland amphibolites are plotted as *triangles; shaded line* depicts the trend of the metamorphic zoning of the Patom Highland amphibolites

ters are applied to construct the diagram in the following coordinates: the An content in Pl versus the Al content in Ca–Am (Fig. 5). Isobares in the diagram are delineated according to variation of Al content in Ca–Am in dependence on both P and T, while isothermes are plotted after An content in Pl. Thus, the plotting of coexisting Ca–Am and Pl compositions determines the PT-conditions of their equilibrium. The resolution of this geothermobarometer depends on the analytical uncertainty in the compositions of Am and Pl. Using an accuracy ± 1.0 mole % Al and Ca in Am and Pl, the standard deviation in the P estimate is ± 1 kb and in the T $\pm 10-15°$, including also the experimental uncertainties.

The compositions of coexisting Hb and Pl from the Patom Highland amphibolites (Petrov, Makrygina 1975) are represented in the resulting diagram to demonstrate the application of this geothermobarometer. These rocks were choosen because the PT-conditions of their formation have been defined by analyses of gaseous – liquid inclusions. According to the latter, the temperature range of the retrograde epidote-amphibolite facies at $P=4.5$–5 kb is 430–480° C. Using our diagram the following PT-parameters have been received for the same assemblages: $P=4.4$–6 kb, $T=450$–480° C. The prograde amphibolite facies according to previous data (Petrov and Makrygina, 1975) is characterised by the T from 540 to 580° C at $P=8$ kb, and after the diagram (Fig. 5) it is estimated at $T=530$–560° and $P=6.2$–7.8 kb. A comparison of these values depict a satisfactory agreement of estimations, received by two independent ways.

Moreover, the diagram has been used for analysis of coexisting Ca–Am and Pl in mafic schists from Vermont to estimate the variation in physical conditions under which they crystallized. In accordance with Laird (1980), there are zones of low (I), medium (II) and high (III)-pressure. Inside each zone a specific prograde metamorphic zonation is observed. Mineral compositional variations in the low-pressure facies series form the biotite-albite (1), biotite-oligoclase (2), garnet-oligoclase-andesine (3) and bytownite-sillimanite (4) zones. Progressive metamorphic zoning at medium pressure is similar to that at low pressure, however, the discontinuous change in Pl composition from Ab to Ol occurs in the garnet subzone: biotite-albite (5), garnet-albite (6), garnet-oligoclase (7) and staurolite-kyanite-oligoclase (8) subzones. In the high-pressure facies series mafic schist, biotite-albite (9) and garnet-albite (10) with omphacite and glaucophane subzones are distinguished. All mentioned zones include the assemblage – Ca–Am+Pl+Ep+Chl+Cc+Q, therefore, we have a favourable opportunity to apply the experimental Pl–Hb geothermobarometer to analyze the PT-conditions of progressive polymetamorphism of the Vermont mafic schists. The compositions of coexisting Am and Pl from all zones were plotted on the considered diagram (Fig. 5), and the PT-paths of the described zonation are outlined.

Thus, the present Hb–Pl geothermobarometer allows to correlate metamorphic zones in metapelites and adjacent metabasites more reliably. However, an application of this geothermobarometer is recommended to amphibolites containing either Zo or Ep. A few tentative experiments employing the Zoisite-free starting mixture revealed a decrease in Al content of residual Am, approximately in range 2–3 wt. %. The reason of this difference is clear: in fact, the Zo, or Ep, presence is a control of a bulk composition, as regards to the Al content, of initial rocks, for those the reported geothermobarometer may be used. Then, the application of the Pl–Hb geothermobarometer to metabasites of the Ufaley metamorphic complex (Likhoidov et al. 1981), represented by the intermittent garnet-bearing and garnet-free zoisite amphibolites, had allowed us to receive the same PT-values of formation of both rock species. So, it seems that Hb+Pl+Zo is the major limiting assemblage. It must be mentioned also, that application of the Pl–Hb geothermobarometer is limited to calciferous and subcalciferous Ams, containing more than 1.50 Ca, less than 1.00 Na, because of an increasing glaucophane-end member in Am it is accompanied by an essential decrease in An content of Pl.

A clinopyroxene (Cpx) appearance in amphibolites with increasing temperature causes a visible change in compositions coexisting Hb and Pl, but it occurs over an upper thermal boundary of epidote amphibolite stability field, fixed by the reaction Hb+Zo+Cc+Q$\rightleftharpoons$Cpx+Pl+H_2O+CO_2, that is experimentally studied now. According to preliminary experimental data this reaction boundary confines the Hb+Zo assemblage stability field by temperatures of about 600° C at $P_{fl}=2$ kb, 622° at $P_{fl}=4$ kb and 635° C at $P_{fl}=6$ kb (at $X_{CO_2}=0.1$) in the iron-free system.

Besides, one must be sure that an examined Hb–Pl assemblage is syngenetic. Undoubtedly, Ca–Am zonal crystals require a particular caution to choose the equilibrium compositions for providing additional evidence in possible conditions of metamorphism. Numerous data about widespread zoning of Am and Pl in metamorphic rocks convince us that trustworthy evidences might be recieved by only an electron microprobe analysis.

Acknowledgments. The author wishes to thank Acad. D.S. Korzhinskii, Dr. L.L. Perchuk and Dr. V.I. Fonarev for the helpful suggestions and constructive criticism.

References

Best NF (1978) A preliminary study of the tremolite-edenite solid solution series. Natur Environ Res Counc Publs Ser 11:162–163

Compton RR (1958) Significance of amphibole paragenesis in the Bidwell Bai Region, California. Am Mineral 43:890–907

Cooper AF (1972) Progressive metamorphism of metabasic rocks from Haast Schist Group of Southern New Zealand. J Petrol 13:457–492

Fonarev VI, Korolkov GYa (1980) The assemblage orthopyroxene + cummingtonite + quartz. The low-temperature stability limit. Contrib Mineral Petrol 73:413–420

Graham CM (1974) Metabasic amphiboles of the Scottish Dalradian. Contrib Mineral Petrol 47:163–185

Grapes RH (1975) Actinolite-hornblende pairs in metamorphosed gabbro, Hidaka Mountains, Hokkaido, Contrib Mineral Petrol 49:125–140

Grapes RH (1977) Chemical inhomogeneity of amphiboles in relation to section orientation in routine EPMA analyses. Geochem J 11:253–255

Grapes RH, Graham CM (1978) The actinolite-hornblende series in metabasites and so-called miscibility gap. Lithos 11:85–97

Hietanen A (1974) Amphiboles pairs, epidote minerals, chlorite and plagioclase in metamorphic rocks, Northern Sierra-Nevada, California. Am Mineral 59:22–40

Klein C (1969) Two amphibole assemblages in the system actinolite-hornblende-glaucophane. Am Mineral 54:113–118

Kostyuk EA (1970) Statystical analyses and paragenetic type of the metamorphic amphiboles. Nauka, Moscow (in Russian)

Laird J (1980) Phase equilibria in mafic shist from Vermont. J Petrol 26:1–38

Leake BE (1962) On the non-existance of a vacant area in the Hallimond calciferous amphibole diagram. Japan J Geol Geophys 33:1–13

Likhoidov GG, Pluysnina LP, Mischenchuk GA (1981) PT-conditions of formation of the Ufaley metamorphic complex amphibolites. Contrib USSR Acad Sci, Ser Geol, No 9:14–25 (in Russian)

Liou JG, Kunyioshi K, Ito K (1974) Experimental studies of the phase relations between greenschist and amphibolite in a basaltic system. Am J Sci 274:613–632

Perchuk LL (1970) Equilibria of rock-forming minerals. Nauka, Moscow (in Russian)

Petrov BV, Makrygina VA (1975) Geochemistry of regional metamorphism and ultrametamorphism. Nauka, Moscow (in Russian)

Raase P (1974) Al and Ti contents of hornblende as indicator of pressure and temperature of regional metamorphism. Contrib Mineral Petrol 45:231–236

Shido F (1958) Plutonic and metamorphic rocks of the Nakoso and Iriton district in the Central Abukuma Plateau. Tokyo Fac Sci J 11:31–127

Shido F, Miyashiro A (1959) Hornblende of basic metamorphic rocks. Tokyi Fac Sci J 12:85–102

Wenk E, Keller F (1969) Isograde in Amphibolitserien der Zentralalpen, Schweiz. Mineral Petrogr Mitt 49:157–198

Received September 24, 1981; Accepted June 11, 1982